Printed Circuit Transmission-Line Characteristic Impedance by Transverse Modal Analysis

HUNG-YUET YEE, SENIOR MEMBER, IEEE, AND KUANG WU, MEMBER, IEEE

Abstract — **Dispersion characteristics of printed circuit transmission lines such as finlines, shielded microstrips, slotlines, suspended striplines, coupled slotlines, and coupled striplines computed by the transverse modal analysis were reported in a previous paper [1]. Application of the transverse modal analysis to compute the characteristic impedances of these printed circuit transmission lines is illustrated in this paper. Favorable comparison with various published data demonstrates the outstanding accuracy achieved by this technique. Combining the characteristic impedance computation with the dispersion results, the transverse modal analysis can be employed for solving various problems in printed circuit transmission lines.**

I. Introduction

APPLICATION of the transverse modal analysis (TMA) to compute the dispersion characteristics of printed circuit transmission lines such as finlines, shielded microstrips, slotlines, suspended striplines, and two-coupled striplines and slotlines was reported in a previous paper [1]. Favorable comparison with results computed by various numerical techniques applied to the same problems verifies the accuracy of the transverse modal analysis solutions.

In addition to the dispersion relationship, the characteristic impedance of a transmission line is another important parameter for microwave designers. Cohn [2] applied the transverse analysis to compute the slot line impedance by first computing the gap capacitance. Sorrentino *et al.* [3] extended the solution to coplanar coupled slot lines with dielectric substrates. In this paper, the transverse modal analysis is generalized to include the computation of the characteristic impedances of finlines, microstrips, and broadside-coupled striplines. The characteristic impedances of similar printed circuit transmission-line systems can be computed in the same manner. Excellent agreement with published results further confirms that this technique is indeed a viable tool for many microwave engineering problems.

Applying the transverse modal analysis as outlined in [1] to a transmission-line cavity, the cavity field distribution and resonant frequency can be computed. The modal series representations are good approximations of the transmission-line fields in various regions if a sufficient number of modes are included. At resonant frequency, the cavity field can be resolved into two components, one representing the transmission-line forward-propagating field and the other representing the backward-propagating field. Either forward or backward propagation can be used to compute the power associated with the transmission-line field by integrating the suitable Poynting vector over the cross section of the transmission-line system. Using this computed power with suitable impedance definitions, the characteristic impedances of various transmission lines can be computed with sufficient accuracy for most engineering applications.

The convergent phenomena in the computation of the characteristic impedance are similar to those for the dispersion relationship. Using the ratio of maximum waveguide mode index to maximum slot aperture or the stripline current mode index, equal to the ratio of waveguide width to aperture or stripline width, correct convergent results are obtained. Detailed discussions on this type of relative convergence can be found in [4]–[6].

II. Formulation

Formulation of characteristic impedances for shielded slotlines (or bilateral finlines) and shielded microstrips (or broadside-coupled striplines) will be considered in detail to illustrate this technique. Using these two guideline examples, characteristic impedances of various printed circuit transmission-line systems can be computed by transverse modal analysis.

With reference to the configuration in Fig. 1 and using the transverse modal analysis method as described in [1], we consider that the shielded slot line or microstrip cavity consists of two rectangular waveguide sections, where the propagation is along the z direction. These two waveguide sections are joined by a window or a strip conductor at $z = g$ and are terminated by an electric wall at $z = h$ and by an electric or magnetic wall at $z = 0$, depending on the required geometry. The transverse field components in the two rectangular waveguide sections are expressed in terms of the rectangular waveguide modal functions as follows.

For region 1 ($g > z > 0$)

$$\boldsymbol{E}_t = \sum_n A_n \boldsymbol{\Phi}_n \left[\begin{matrix} \sin \\ \cos \end{matrix} (\beta_n z) \right] \tag{1a}$$

Manuscript received October 9, 1985; revised May 9, 1986.

The authors are with the Antenna Laboratory, Texas Instruments, Inc., P.O. Box 869305, Plano, TX 75086.

IEEE Log Number 8610287.

0018-9480/86/1100-1157$01.00 ©1986 IEEE

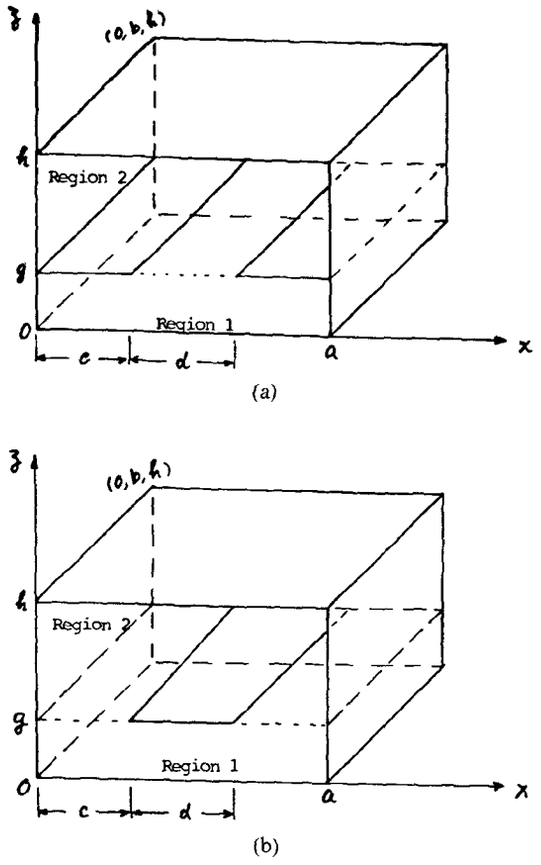

Fig. 1. Schematic diagram of two-dielectric-layer cavity. (a) Finline. (b) Shielded microstrip.

$$\boldsymbol{H}_t = j\sum_n A_n Y_n \hat{z} \times \boldsymbol{\Phi}_n \begin{bmatrix} \cos \\ -\sin \end{bmatrix} (\beta_n z). \tag{1b}$$

For region 2 ($h > z > g$)

$$\boldsymbol{E}_t = \sum_n B_n \boldsymbol{\Phi}_n \sin\left[\beta_n'(h-z)\right] \tag{2a}$$

$$\boldsymbol{H}_t = j\sum B_n Y_n' \hat{z} \times \boldsymbol{\Phi}_n \cos\left[\beta_n'(h-z)\right] \tag{2b}$$

where the upper and lower functions are applied to the electric and magnetic wall at $z = 0$, respectively; n is the compound index, which represents two index numbers plus an index indicating the TE or TM mode; and $\boldsymbol{\Phi}_n$ is the normalized waveguide modal function. The wave admittance Y_n is related to the z propagation constant β_n by $Y_n = \beta_n/\omega\mu$ for TE modes and $Y_n = \omega\epsilon/\beta_n$ for TM modes, where ω is the angular frequency and μ and ϵ are the permeability and permittivity, respectively. Conveniently assuming that the y variation index is equal to one, the z propagation constants are given by

$$\begin{bmatrix} \beta_n \\ \beta_n' \end{bmatrix} = \left\{ k_0^2 \begin{bmatrix} \epsilon_r \\ \epsilon_r' \end{bmatrix} - (n\pi/a)^2 - (\pi/b)^2 \right\}^{1/2} \tag{3}$$

where ϵ_r and ϵ_r' are the relative dielectric constants in regions 1 and 2, respectively.

Following the same procedures as employed in the dispersion computations, the electric field in the finline slot aperture is assumed to be

$$\boldsymbol{E}_a = \sum_q C_q \boldsymbol{\Omega}_q \tag{4}$$

and the surface current density on the microstrip conductor is represented by

$$\boldsymbol{J} = j\sum_q C_q \boldsymbol{v}_q \tag{5}$$

where the aperture field modal function $\boldsymbol{\Omega}_q$ and strip current modal function $\boldsymbol{v}_q$ are defined in [1] and will not be repeated here.

Enforcing the boundary conditions on the cavity interface and using the Galerkin's method, the following matrix equation is derived from the above equations:

$$[M][C] = 0 \tag{6}$$

where

$$M_{pq} = \sum_n W_{qn} W_{pn} \begin{cases} G_n & \text{for finline} \\ 1/G_n & \text{for microstrip} \end{cases}$$

$$G_n = Y_n' \cot\left[\beta_n'(h-g)\right] + Y_n \begin{bmatrix} \cot \\ -\tan \end{bmatrix} (\beta_n g)$$

$$W_{pn} = \int \begin{bmatrix} \boldsymbol{\Omega}_n \\ \boldsymbol{v}_n \end{bmatrix} \cdot \boldsymbol{\Phi}_n \, dS.$$

The surface integration of the above integral is integrated over the slot aperture for a finline and over the strip conductor for a microstrip. In order to obtain a set of nontrivial coefficients, the determinant of the square matrix given by (6) must vanish. This requirement determines the cavity resonant frequency and, hence, the dispersion characteristics. Substituting the computed resonant frequency into (6), the slot aperture field or the strip current expansion coefficients and, hence, the cavity field can be computed.

The rectangular waveguide vectorial modal functions for TE and TM modes are given by Marcuvitz [7] as follows:

$$\Psi_n = \begin{matrix} \cos \\ \sin \end{matrix} (n\pi x/a) \begin{matrix} \cos \\ \sin \end{matrix} (\pi y/b) \qquad \begin{matrix} \text{for TE mode} \\ \text{for TM mode} \end{matrix}$$

$$\boldsymbol{\Phi}_n = (N_n/\pi) \begin{cases} \hat{z} \times \nabla \Psi_n & \text{for TE mode} \\ \nabla \Psi_n & \text{for TM mode} \end{cases}$$

$$N_n = (2\Delta_n/ab)^{1/2}(\pi/k_c)$$

$$\Delta_n = \begin{cases} 1 & \text{if } n = 0 \\ 2 & \text{if } n \neq 0 \end{cases}$$

$$k_c/\pi = \left[(n/a)^2 + (1/b)^2\right]^{1/2}$$

where TE and TM refer to the transverse electric and transverse magnetic fields with respect to the z axis, respectively. For characteristic impedance computation, the power propagating along the y direction is required, and, hence, the z components of the electric and magnetic fields. To be consistent with (1), the z components of the cavity field in region 1 may be written as

$$H_z = \sum_n A_n (k_c/\pi)^2 (N_n/j\omega\mu) \Psi_n \begin{bmatrix} \sin \\ \cos \end{bmatrix} (\beta_n z) \tag{7a}$$

for TE modes, and as

$$E_z = -\sum_n A_n (k_c/\pi)^2 (N_n/\omega\mu)\Psi_n \begin{bmatrix} \cos \\ -\sin \end{bmatrix} (\beta_n z) \quad (7b)$$

for TM modes. Equations (7a) and (7b) are applicable to region 2, provided that A is replaced by B, and the functions inside the square brackets are replaced by $\cos[\beta_n'(h-z)]$ and $\sin[\beta_n'(h-z)]$, respectively.

To compute the y-propagating transmission-line power, the y dependents in (1) and (7) are resolved into two terms: one for positive y propagation and the other for negative y propagation. Either positive or negative y-propagating field can be chosen to compute the transmission-line power and the characteristic impedance. Attention must be given to the transmission-line power computation which requires the cross-coupled TE and TM modal fields.

The power associated with the transmission-line mode can be computed by integrating the Poynting vector

$$\boldsymbol{p} = \boldsymbol{E} \times \boldsymbol{H}^*/2$$

over the transmission-line cross section on any plane normal to the y axis. The resultant modal power in region 1 (having the same modal index) with magnetic wall at $y = 0$ is given by

$$P_n = [\pi/(8\omega\mu b)]\Big\{|D_{n_1}|^2/b + nD_{n_1}^* D_{n_2}/a\Big)Q_n^{\mp} + \delta_n\Big[\Big((|D_{n_2}|^2/b\Big)(k/\beta_n)^2 - \big(nD_{n_1}^* D_{n_2}/a\big)(\beta_n^*/\beta_n)\Big]Q_n^{\pm}\Big\} \quad (8a)$$

$$Q_n^{\pm} = (g/2)|\sec^2(\beta_n g) + \tan(\beta_n g)/(\beta_n g)| \quad (8b)$$

$$D_{ni} = \sum_q C_q W_{qni}, \qquad i = 1 \text{ or } 2 \quad (8c)$$

$$\delta_n = \begin{cases} 0 & \text{if } n \neq 0 \\ 1 & \text{if } n = 0 \end{cases}$$

where the subscript $i = 1$ or 2 indicates the quantity for the TE or TM mode solution obtained from the matrix equation (6) and * indicates the complex conjugate quantity. For the electric wall at $y = 0$, (8) is applicable provided that (8b) is replaced by

$$Q_n^{\pm} = (g/2)|\csc^2(\beta_n g) - \cot(\beta_n g)/(\beta_n g)|. \quad (9)$$

The modal power in region 2, P_n', can be expressed by (8) provided that β_n is replaced by β_n', ϵ_r by ϵ_r', and (9) replaced by

$$Q_n^{\pm} = [(h-g)/2]|\csc^2[\beta_n'(h-g)] - \cot[\beta_n'(h-g)]/[\beta_n'(h-g)]|. \quad (10)$$

We are now ready to compute the total power associated with the transmission-line mode by summing all the modal powers in both regions 1 and 2

$$P = \sum_n (P_n + P_n'). \quad (11)$$

Using the total power obtained by (11), the characteristic impedances based on power definition can be computed as shown in the next section.

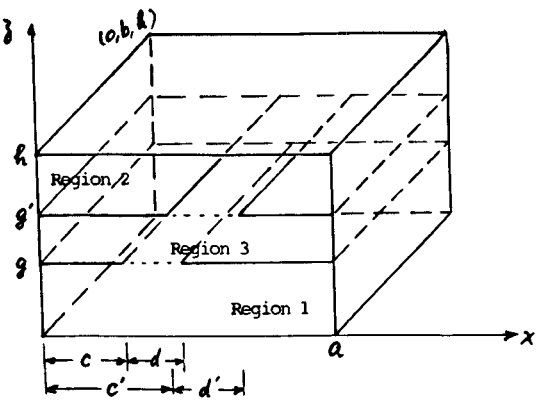

Fig. 2. Schematic diagram of three-dielectric-layer cavity. (a) Shielded two slotlines. (b) Shielded two striplines.

III. Characteristic Impedances

The characteristic impedance of a conventional two-conductor transmission line is defined by

$$Z_c = 2P/|I|^2 \quad (12)$$

where P is the total power transferred across the reference transverse plane and I is the total longitudinal current carried by one conductor. This definition is easily applied to microstrips with no ambiguity. This definition is also used for a two-coupled stripline, as shown in Fig. 2(b), if $d = d'$. On the other hand, the characteristic impedance of a conventional slotline may be defined as

$$Z_c = |V|^2/(2P) \quad (13)$$

where V is the voltage across the slot. This definition is also used for the bilateral finline, as shown in Fig. 2(a), with $d = d'$ and $c = c'$.

To compute the microstrip current and the finline voltage, the modal expressions must be resolved into two terms in the same manner as in the power computation. After the modal coefficients of the aperture field and the strip current are determined for a given resonant frequency, the voltage across the slot and the total longitudinal strip current can be easily computed by the integration of (4) and (5) across the slot aperture and the strip conductor, as

given by

$$V = \int_c^{c+d} \boldsymbol{E}_{at} \cdot \hat{\boldsymbol{x}}\, dx$$

$$I = \int_c^{c+d} \boldsymbol{J}_t \cdot \hat{\boldsymbol{y}}\, dx.$$

Here, the subscript t indicates the aperture electric field and the strip current density associated with the transmission line. The characteristic impedances of the microstrip and the finline can be computed by substituting these results into (12) and (13).

IV. Numerical Results

The accuracy of the numerical solution computed by the transverse modal analysis depends on the way in which the infinite series representations of the fields in the cavity are truncated. Using the ratio of maximum waveguide mode index to maximum slot aperture or the stripline current mode index, which is equal to the ratio of waveguide width to aperture or stripline width, correct convergent results are obtained. This relative convergence is identical to that discussed in [4]–[6] and is verified by two examples given in this section.

To illustrate the accuracy of the characteristic impedance computed by TMA, solutions of bilateral finlines, shielded microstrip, rectangular coaxial lines, and two broadside-coupled striplines are considered here. The rectangular coaxial line is a special case of the shielded microstrip where the relative dielectric constants are identical in both regions.

The schematic diagram of the bilateral finline under consideration is shown in Fig. 1(a) with magnetic wall at $z = 0$. The parameters are given as follows:

Waveguide dimensions	0.28 by 0.14 in,
Dielectric slab	thickness = 0.00492 in, relative dielectric constant = 3.0,
Slot width	0.0197 in.

Fig. 3 shows the computed characteristic impedances of the finline with 0.5-mm slot width using ratios of maximum slot mode index to waveguide mode index equal to 1/8 and 1/4 at frequencies equal to 29.3 and 30.0 GHz, respectively. The ratio of slot width to waveguide width is equal to 1 : 7.11. Observe that by using a modal ratio equal to 1/8, the numerical result converges rapidly to 403 Ω, which compares favorably with that computed by Schmidt and Itoh using the spectral domain (SD) technique [8]. However, the computed impedance approaches the wrong value when the modal ratio is equal to 1/4, which is greater than the suitable ratio.

Compared in Fig. 4 are results computed by the transverse modal analysis and those presented by Schmidt and Itoh. Excellent agreement between these two sets of data is observed over a broad range of frequencies.

Characteristic impedances of microstrips have been investigated by many authors [9], [10]. Practical applications require shielded microstrips to avoid the leakage of electromagnetic power. The TMA technique is highly suitable for these applications. It is well known that the field is highly concentrated underneath the strip conductor in the presence of a dielectric substrate. The shielded microstrip solution is a good approximation to the open version if the walls are sufficiently far away from the strip conductor.

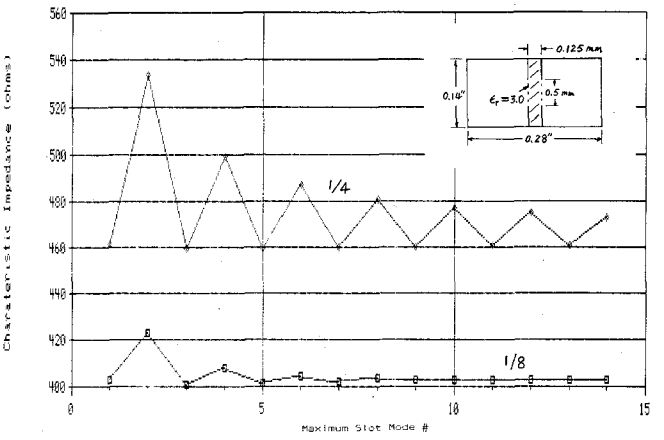

Fig. 3. Finline characteristic impedance by TMA using mode ratio = 1/8 and 1/4. Waveguide dimensions; 0.28 in by 0.14 in; slot width, 0.0197 in; dielectric slab thickness, 0.00492 in; dielectric constant, 3.0.

Consider a microstrip where the waveguide dimensions are 2.0 by 0.6 in, the strip width is 0.2 in, the dielectric slab thickness is 0.1 in, and the relative dielectric constant is 9.6. Depicted in Fig. 5 are the TMA characteristic impedances computed by mode ratios equal 1/10 and 1/5. The solution with the mode ratio equal to 1/10 (the suitable ratio) converges to 33.1 Ω, which compares favorably with the 32.8 Ω computed by Farrar and Adams [6] using the potential theory (PT) method for covered microstrips without two side walls.

Listed in Table I are microstrip characteristic impedances computed by the TMA and PT methods. The solution obtained by the PT technique is computed in the absence of two side walls. Compared in Table II are microstrip characteristic impedances computed by TMA, the moment method (MM), and conformal mapping (CM) [11]. No shielding structure is used for the MM and CM computed results. Observe that the TMA solution compares very well with results computed by various techniques. In the narrow-strip case, where $d/g = 0.1$, the field distribution spreads far into the waveguide region and the computed characteristic impedance is smaller than in the unshielded microstrip. In general, smaller side-wall or top-wall spacing results in a smaller characteristic impedance.

It is interesting to observe that the microstrip characteristic impedances computed by TMA vary very slightly with frequency in the low-frequency domain, where the quasi-TEM solution is valid.

A rectangular coaxial line is a special case of a shielded microstrip where the rectangular waveguide is filled with a uniform dielectric medium. The numerical data shown in Fig. 6 were computed for symmetrical rectangular coaxial lines only, while the equations derived in the previous section are applicable to coaxial lines with offset inner

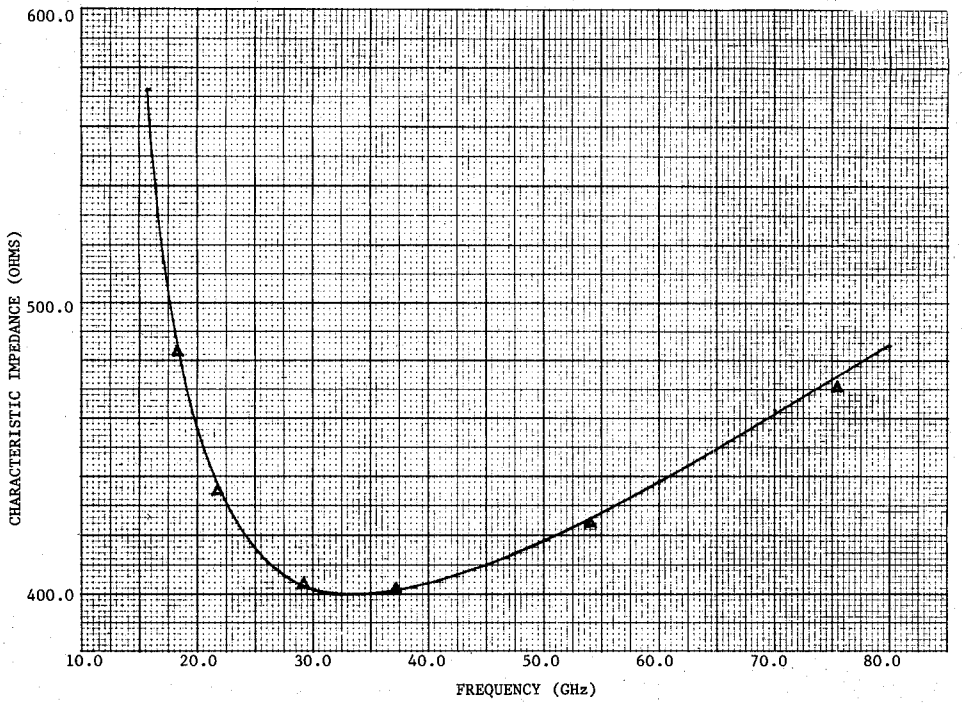

Fig. 4. Comparison of finline characteristic impedances by SD (solid curve) and TMA (triangular dot). Geometric configuration is the same as in Fig. 3.

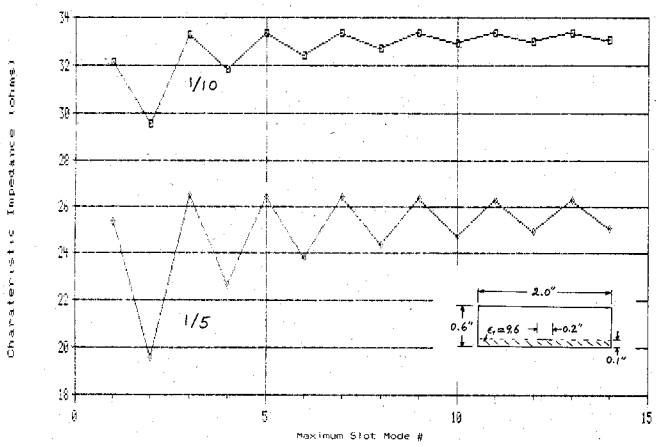

Fig. 5. Shielded microstrip characteristic impedance by TMA using mode ratio = 1/10 and 1/5. Waveguide dimensions, 2.0 in by 0.6 in; strip width, 0.2 in; dielectric slab thickness, 0.1 in; dielectric constant 9.6.

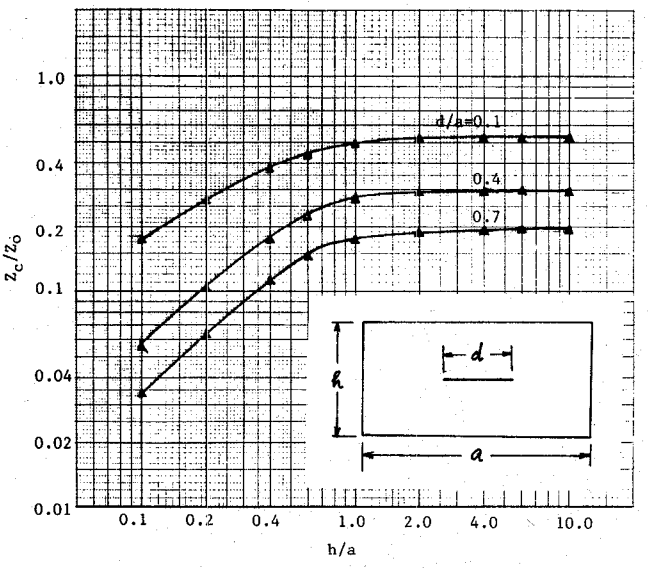

Fig. 6. Comparison of rectangular coaxial line characteristic impedances by SIE (solid curves) and TMA (triangular dots). Z_c: characteristic impedance; Z_0: intrinsic impedance.

TABLE I
COMPARISON OF MICROSTRIP CHARACTERISTIC IMPEDANCES FOR $h/g = 6$ AND DIELECTRIC CONSTANT = 9.6

a/d	d/g	TMA	PT
10.0	0.4	69.7	70.9
10.0	0.8	53.8	53.9
6.0	1.0	47.9	48.5
10.0	1.0	48.4	48.5
10.0	2.0	33.1	32.8

TABLE II
COMPARISON OF MICROSTRIP CHARACTERISTIC IMPEDANCES FOR $h/g = 10.0$ AND DIELECTRIC CONSTANT = 6.0

a/d	d/g	TMA	MM	CM
10.0	0.1	102.92	135.46	134.35
40.0	0.1	128.96	135.46	134.35
10.0	0.4	86.30	91.17	89.91
10.0	1.0	60.49	62.71	60.97
10.0	4.0	25.99	27.30	26.03

conductors. Also shown in Fig. 6 are results computed by Tippet and Chang [11] using the singular integral equation (SIE) technique. Excellent agreement is observed for various combinations of waveguide dimensions and strip conductors, as indicated in the figure. The transmission-line guided wavelength computed by the TMA method is equal to the exact transmission-line solution for any combination of geometric parameters.

Following the same techniques as outlined in [1] and in the previous section, characteristic impedances of the shielded two-coupled strips shown in Fig. 2 and of similar printed circuit transmission lines can be analyzed by TMA.

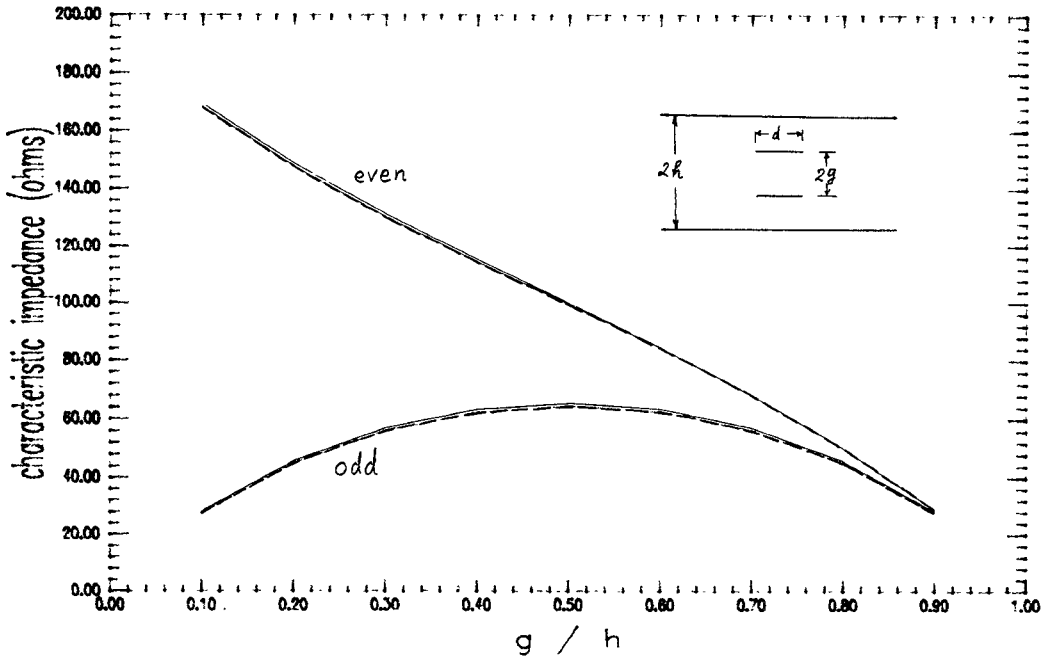

Fig. 7. Comparison of characteristic impedances of two broadsidecoupled strips by Cohn [7] (——) and TMA (-----) for $h/d=1$.

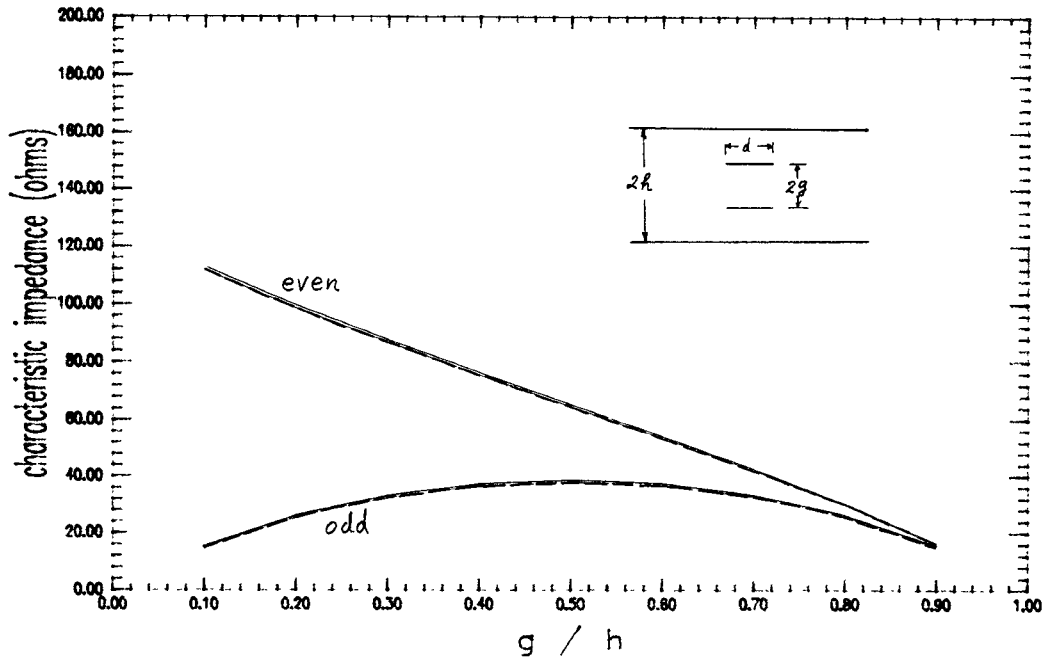

Fig. 8. Comparison of characteristic impedances of two broadsidecoupled strips by Cohn [7] (——) and TMA (-----) for $h/d=0.5$.

For the special case of two identical broadside-coupled strips, the odd- and even-mode characteristic impedances can be computed by the microstrip solution with the electric and magnetic walls at $z=0$, respectively. The TMA results are shown in Figs. 7 and 8.

Also shown in Figs. 7 and 8 are results computed by Cohn [12] using the conformal mapping technique. In order to compare the TMA solutions with those computed by Cohn, the side-wall spacing is chosen to be ten times the stripline width. For all cases shown in Figs. 7 and 8, the field is negligible at the side wall locations even without the side walls. Excellent agreement is observed over a wide range of parameters. This comparison and that in Figs. 4 and 6 show that excellent accuracy can be achieved by TMA for printed circuit transmission lines.

V. Conclusions

Characteristic impedances of printed circuit transmission lines computed by the transverse modal analysis technique are illustrated in this paper. Equations are derived only for the finlines and shielded microstrips. It is easy to

extend the applications to other printed circuit transmission-line configurations. Favorable comparison with results computed by various techniques, such as spectral domain, moment method, conformal mapping, and potential method, demonstrates the accuracy achievable by TMA. Combined with the dispersion formulation discussed in [1], the transverse modal analysis is a viable tool for the design of printed circuit transmission lines where both the dispersion and characteristic impedance are important parameters.

The advantages of the TMA technique are its application to the high-frequency domain, where higher order modes may propagate, and its simple formulation and computation for similar transmission-line configurations. Although only a thin-conductor formulation is derived in this paper, extension to include the effects of finite-thickness conductors can be obtained with no difficulty.

References

[1] H. Y. Yee, "Transverse modal analysis for printed circuit transmission lines," *IEEE Trans. Microwave Theory Tech.*, vol. MTT-33, pp. 808–816, 1985.

[2] S. B. Cohn, "Slotline on dielectric substrate," *IEEE Trans. Microwave Theory Tech.*, vol. MTT-17, pp. 768–778, 1969.

[3] R. Sorrentino, G. Leuzzi, and A. Silbermann, "Characteristics of metal–insulator–semiconductor waveguides for monolithic microwave circuits," *IEEE Trans. Microwave Theory Tech.*, vol. MTT-32, pp. 410–416, 1984.

[4] S. W. Lee, W. R. Jones, and J. Campbell, "Convergence of numerical solutions of iris-type discontinuity problems," *IEEE Trans. Microwave Theory Tech.*, vol. MTT-19, pp. 528–536, 1971.

[5] R. Mittra, T. Ioh, and T.-S. Li, "Analytical and numerical studies of the relative convergence phenomenon arising in the solution of an integral equation by moment method," *IEEE Trans. Microwave Theory Tech.*, vol. MTT-20, pp. 96–104, 1972.

[6] M. Leroy, "On the convergence of numerical results in modal analysis," *IEEE Trans. Antennas Propagat.*, vol. AP-31, pp. 655–659, 1983.

[7] N. Marcuvitz, *Waveguide Handbook*. New York: McGraw-Hill, 1950, ch. 5.

[8] L.-P. Schmidt and T. Itoh, "Spectral-domain analysis of dominant and high order modes in fin-line," *IEEE Trans. Microwave Theory Tech.*, vol. MTT-28, pp. 981–985, 1980.

[9] S. B. Cohn, "Characteristic impedance of the shielded-strip transmission line," *IRE Trans. Microwave Theory Tech.*, vol. MTT-2, pp. 52–57, 1954.

[10] H. A. Wheeler, "Transmission line properties of parallel strips separated by a dielectric sheet," *IEEE Trans. Microwave Theory Tech.*, vol. MTT-13, pp. 172–185, 1965.

[11] A. Farrar and A. T. Adams, "A potential theory method for covered microstrip," *IEEE Trans. Microwave Theory Tech.*, vol. MTT-21, pp. 494–496, 1973.

[12] A. Farrar and A. T. Adams, "Characteristic impedance of microstrip by the method of moments," *IEEE Trans. Microwave Theory Tech.*, vol. MTT-18, pp. 65–66, 1970.

[13] S. B. Cohn, "Characteristic impedances of broadside-coupled strip transmission lines," *IEEE Trans. Microwave Theory Tech.*, vol. MTT-8, pp. 633–637, 1960.

Hung-Yuet Yee (SM'70) received the Ph.D. degree in electrophysics from the Polytechnic Institute of New York in 1968.

From July 1963 to February 1966, he was a Research Associate with the University of Alabama Research Institute, Huntsville, AL. From July 1968 to August 1971, he was a Senior Research Associate and Assistant Professor with the University of Alabama in Huntsville. In August 1971, he joined the staff of Texas Instruments, Inc., and was assigned to the Antenna Laboratory. Since 1979, he has been a Senior Member of the Technical Staff.

Kuang Wu (S'82–M'83) was born in Taoyuan, Taiwan, China, on March 13, 1950. He received the B.S. and M.S. degrees in physics from Fu-Jen Catholic University, Taipei, Taiwan, China, in 1972 and the M.S. degree, also in physics, from Mississippi State University in 1977. In 1983, he received the Ph.D. degree in electrical engineering from North Carolina State University.

From 1978 to 1979, he was a dispersion engineer at McDonnell Douglas Technical Services Co., Houston, TX. He joined Texas Instruments, Inc., in 1983 and is now a Visiting Professor of electrical engineering at Ta-Tung Institute of Technology, Taipei, Taiwan, China. His professional interests include the areas of analytical and numerical electromagnetics.